PHYSICAL REVIEW B VOLUME 57, NUMBER 9 1 MARCH 1998-I

Pressure-induced phase transitions in silver halides

G. S. Nunes and P. B. Allen
Department of Physics, SUNY at Stony Brook, Stony Brook, New York 11794-3800

José Luís Martins
Departamento de Física, Instituto Superior Técnico, Avenida Rovisco Pais 1, 1096 Lisboa, Portugal
and Instituto de Engenharia de Sistemas e Computadores, Rua Alves Redol 9, 1000 Lisboa, Portugal

(Received 2 September 1997)

A first-principles study of the relative stability of a few different structures, viz. AgCl, AgBr, and AgI, is undertaken. Modern pseudopotentials, the local-density approximation, and a plane-wave basis are used. The relative stability of the cubic zinc blende, rocksalt, and CsCl structures, as well as the wurtzite, β-Sn, NiAs, and cinnabar structures is investigated. Ground-state structural parameters are computed and compared with experiment. The optimization of the cinnabar structure leads to a simple rhombohedral phase, which is found to be the most stable among those considered in an intermediate range of pressures for AgCl and AgBr. According to these results, AgCl and AgBr prefer a rhombohedral route from the rocksalt structure to the CsCl structure instead of the usual discontinuous transition which is common in ionic compounds.
[S0163-1829(98)03309-8]

I. INTRODUCTION

Silver halides are important because of their unique application to the photographic process.[1] They are also very good solid electrolytes.[2]

The silver atom possesses a completely filled $4d$ shell, followed by a lone $5s$ electron which can be transferred to the halide atom. However, there is also hybridization of the silver d states and the halide p states leading to a more complicated electronic structure. In fact, on the Phillips[3] ionicity scale, silver halides lie close to the borderline dividing ionic and covalent compounds; AgCl and AgBr are on the ionic side and AgI is on the covalent side.

Experimentally it is found that the rocksalt structure is preferred for AgCl and AgBr, under atmospheric conditions.[4] Both these compounds have been found by many authors to undergo a first-order transformation around 8–9 GPa.[5,6] Slykhouse and Drickamer found $P_c = 8.7$ GPa for AgCl and $P_c = 8.3$ GPa for AgBr. It was first supposed that this was a transition into the CsCl structure.[5,6] This is the behavior known for alkali halides (e.g., rocksalt itself) which are ionic. Later measurements[7] indicated a transformation into a hexagonal structure. It was conjectured[7] that this was the cinnabar structure.[4] AgI, on the other hand, is found in both the zinc-blende (ZB) and wurtzite phases, associated with covalent compounds,[8] at atmospheric pressure and room temperature. It has an interesting phase diagram, with structural changes occurring at relatively low pressures and temperatures, which signal small energy differences. At low temperatures, the zinc-blende (γ-AgI) and wurtzite (β-AgI) phases change into an intermediate tetragonal phase, at 0.2 GPa, which changes into the rocksalt structure, at 0.4 GPa.[9–11] At a pressure of 9–10 GPa, another transition has been reported.[2,5,6,11] A value of 9.7 GPa was obtained by Riggleman and Drickamer.[12] There is uncertainty in the literature as to the exact nature of the high-pressure phase. The CsCl structure and a tetragonal structure have both been proposed.[6,7]

In this paper, we employ the local-density approximation (LDA) with a pseudopotential plane-wave basis method, to determine the total energies and cohesive energies as a function of volume, for AgCl, AgBr, and AgI in a few structures. These are the three cubic structures, NaCl, zinc blende (ZB), and CsCl, the hexagonal NiAs structure, tetragonal β-Sn structure (for AgBr and AgI), the hexagonal wurtzite structure (for AgI only), and the cinnabar structure.

The present method has also been used successfully by Kirchhof *et al.*[13] to determine the equilibrium properties of AgCl. Chelikowsky[14] has calculated the ZB → NaCl transition pressure for AgI using pseudopotentials but with a Gaussian basis. Gupta and Singh[15] have calculated the NaCl → CsCl using model potentials. We have previously employed the techniques of this work to compute the Kohn-Sham electronic density of states for AgCl, AgBr, and AgI.[16]

II. COMPUTATIONAL TECHNIQUES

We use the local-density approximation of density-functional theory,[17,18] with the exchange-correlation potential of Ceperley and Alder[19] as parametrized by Perdew and Zunger.[20] The core-valence interaction is described by a pseudopotential and the wave functions are expanded in a plane-wave basis set.

The distinction between core and valence electrons is not always sharp. Here, we include the silver $4d$ electrons as valence electrons. This is of fundamental importance in order to accurately describe the hybridization between these states and the halide p states. The $4d$ states of silver are quite localized, requiring efficient pseudopotentials to keep the size of the plane-wave expansion manageable. The size of the effective Hamiltonian ranged from 1500 by 1500 for the CsCl high-pressure structure of AgCl, to 7000 by 7000 for the wurtzite structure in AgI. Diagonalization of such large Hamiltonian matrices is conducted with an iterative scheme.[21] The pseudopotentials are generated using the

TABLE I. The calculated equilibrium structural properties of silver halides, lattice constant a, cohesive energy, CE, bulk modulus, B_0, and its pressure derivative are compared with experiment. NaCl stands for rocksalt and W stands for wurtzite.

		a (Å)	CE (eV)	B_0 (GPa)	B_0'
AgCl(NaCl)	Theory	5.41	6.26	66.8	5.2
	Experiment	5.55[a]	5.56[b]	51.3[c] (0 K)	5.98[f]
AgBr(NaCl)	Theory	5.64	5.90	60.3	5.1
	Experiment	5.75[a]	5.17[b]	41[d] (298 K)	8.5[g]
AgI (ZB)	Theory	6.36	5.78	40.4	5.2
	Experiment	6.47[a]	4.73[b]	24[e] (298 K)	8.5[g]
AgI (W)	Theory	4.49,7.36	5.79	40.5	4.9
	Experiment	4.59,7.50[e]	4.73[b]	24[e] (298 K)	8.5[g]

[a] Reference 4.
[b] References 36,38.
[c] Reference 27.
[d] Reference 35.
[e] Reference 37.
[f] Reference 28.
[g] Reference 34.

Troullier and Martins[22] recipe and equal core radii, r_c, for s, p, and d angular momentum channels. The values of r_c are chosen to be 2.35, 1.65, 1.85, and 2.85 (atomic units), for Ag, Cl, Br, and I, respectively. These semilocal potentials were then converted to the Kleinman-Bylander form,[23] to be used in the plane-wave solid-state calculations. The method of Gonze *et al.*,[24] with a local d channel for chlorine and bromine and a local s channel for silver and iodine, ensured that ''ghost states'' were absent. The convergence with respect to basis set size is dominated by the 4d valence electrons of silver. With an energy cutoff of 60 Ry the total energy is within 0.05 eV/molecule of the values obtained with much larger expansions.

The Brillouin-zone integration is performed with the special **k**-point method with $q_1q_2q_3=444$, in the notation of Monkhorst and Pack,[25] for the cubic structures, the NiAs structure, the β-Sn structure, and also the wurtzite structure. For the cinnabar structure (with six atoms in the unit cell), we have used $q_1q_2q_3=332$ and for the particular case when this structure reduces to rhombohedral (which can be described with two atoms in the unit cell) we use $q_1q_2q_3=666$.

III. ZERO-PRESSURE RESULTS

Equilibrium volumes for the cubic structures were calculated through a Murnaghan[26] fit to $E(V)$, for about seven volumes around the curve minimum. For the wurtzite structure of AgI, we have calculated, for each volume, the energies for 5×4 combinations of c/a and u. The values of c/a and u which minimize the total energy at that volume and the total energy itself are then determined from a quadratic interpolation of those points. Calculated structural parameters are compared in Table I with experiment. The lattice constants are 1 to 2.5% smaller than experiment and the binding energies are 12 to 20% larger than the measured values. These are the typical deviations of local-density calculations. The predicted bulk moduli are 30 to 70 % higher than experiment, a large error when compared to what is expected from local-density calculations. But it has been found for AgCl that the bulk modulus changes from 46 GPa at room temperature to 51 GPa at low temperatures according to ultrasonic velocity measurements, the difference being due to the softening of the c_{11} elastic constants.[27] This indicates a large anharmonicity of the force constants of that phase and a large influence of vibrations in the elastic coefficients. The discrepancy between the calculated and measured values would be reduced if we corrected our results for zero-point motion and made our comparison with low-temperature instead of room-temperature measurements of the bulk moduli of AgBr and AgI. The general trends in the silver halides are correctly predicted by the calculations: larger lattice constant, smaller binding energy, and smaller bulk modulus for the heavier halide compounds.

For β-AgI, we find equilibrium values of 1.64 for c/a and 0.38 for u, very close to the ideal values $\sqrt{8/3}$ and 3/8, and in very good agreement with the experimental figures of 1.635 and 0.375. Also, our value of c/a does not change under compression, which means that under pressure, the wurtzite structure is compressed uniformly until the first discontinuous change occurs. Lawaetz[28] has noticed a correlation between the deviation of c/a from its ideal value and the stability of the wurtzite structure over the zinc-blende structure. He suggests that the wurtzite structure is preferred when this deviation is negative. Here we have found that the c/a deviation is close to zero and the wurtzite and ZB structures are very close to each other in energy. In fact, the calculated difference in energy between wurtzite and zinc blende for AgI of 0.01 eV/molecule is smaller than our numerical accuracy and one should also bear in mind that this figure is also small when compared to the typical accuracy of the LDA itself. The observation of both phases of AgI under ambient conditions confirms the smallness of their energy differences.[4,8]

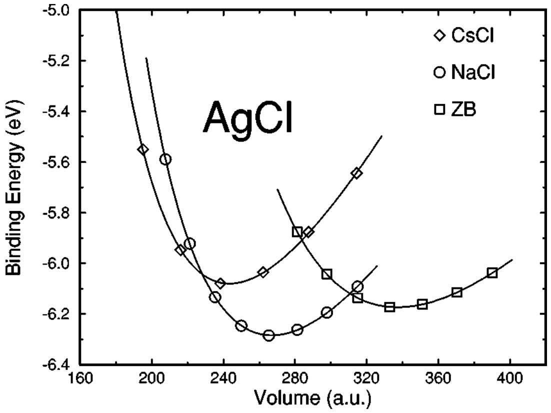

FIG. 1. AgCl: Calculated binding energy in (eV/molecule) for three different crystal structures — CsCl, NaCl and zinc blende (ZB) — as a function of volume in atomic units. Calculated points are shown and the solid line is a Murnaghan fit to these points.

IV. RELATIVE STRUCTURAL STABILITY AND HIGH-PRESSURE PHASES

Figures 1, 2, and 3 show the calculated energy versus volume equation of state, $E=E(V)$, for a few structures, for AgCl, AgBr, and AgI. The Murnaghan form is assumed.[26]. The serious candidate phases for the ground states (zero pressure) of the silver halides are the (cubic) rocksalt and ZB structures. The (hexagonal) wurtzite structure for AgI is also shown (in Fig. 3). We find that the LDA agrees with what is observed in standard atmospheric conditions. For AgCl and AgBr, the rocksalt structure is favored, with the ZB structure higher up by 0.08 and 0.1 eV/molecule, respectively. For AgI, the wurtzite structure, together with the ZB structure, lie lowest in energy, with the rocksalt structure at $0.04-0.05$ eV/molecule higher. So the LDA is predicting the ionic to covalent transition which is observed to occur for silver halides as one proceeds down the halide column.

As candidates for the high-pressure stable phases, we have investigated the cubic CsCl structure, the hexagonal NiAs structure, the tetragonal β-Sn structure, and the cinnabar structure. Our LDA results for some of these structures are also shown in Figs. 1, 2, and 3.

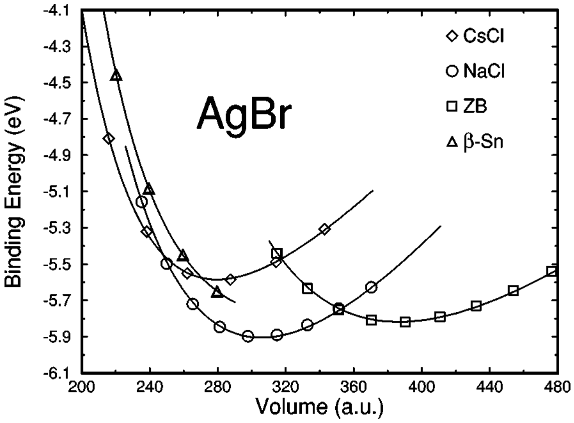

FIG. 2. AgBr: Calculated binding energy in (eV/molecule) for four different crystal structures — CsCl, NaCl, zinc blende (ZB) and β-Sn — as a function of volume in atomic units. Calculated points are shown and the solid line is a Murnaghan fit to these points.

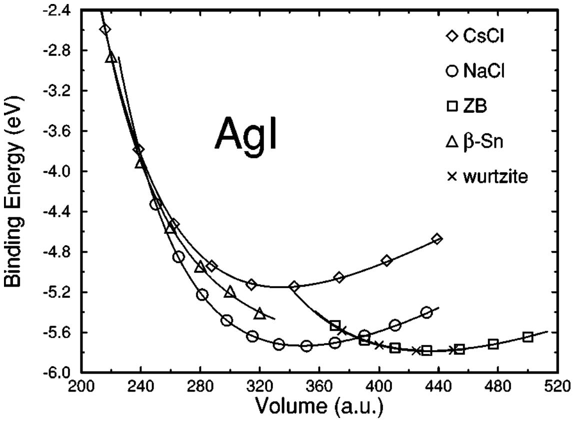

FIG. 3. AgI: Calculated binding energy in (eV/molecule) for five different crystal structures — CsCl, NaCl , ZB, Wurtzite and β-Sn — as a function of volume in atomic units. Filled circles are calculated points and the solid line is a Murnaghan fit to these points.

For AgCl and AgBr, the CsCl structure is clearly favored at high pressures over the other structures shown in Figs. 1 and 2. For AgI, the CsCl structure is still favored up to pressures around 40 GPa (Fig. 3). As discussed later, the consideration of the cinnabar phase changes this simple picture. Our NaCl → CsCl transition pressure for AgCl matches the experimentally found transition pressure fairly well (20% different). But this is not so for the NaCl → CsCl transition in AgBr and especially not so for the NaCl → CsCl transition in AgI (Table II). Gupta and Singh[15] have also calculated these transition pressures with empirical potentials, which contain the (simply ionic) Born-Mayer form plus three body (covalent) terms, with parameters which are fit to a few experimental numbers. These authors agree with the experimental figures and disagree with our *ab initio* results. However there is experimental evidence that the high-pressure phases *do not* have the CsCl structure and our results for the cinnabar structure show that indeed this is probably the case. This suggests that the agreement of Gupta and Singh[15] may be fortuitous and that forces in the silver halides may require more complicated modeling.

The β-Sn structure was calculated, at high pressures, for

TABLE II. Calculated transition pressures, P_c, between pairs of different crystal structures — for AgCl, AgBr, and AgI. Experimentally, for AgCl, a transition from the NaCl structure into an undetermined structure has been measured at 8.7 GPa. Similarly, for AgBr, a transition from the NaCl structure into an undetermined phase has been seen at 8.3 GPa. For AgI, a low-pressure transition into the NaCl structure has been measured at 0.4 GPa and another, from the NaCl structure into an undetermined structure has been measured at 9.7 GPa (Ref. 6).

	Calculated P_c (GPa)	Calculated $\Delta V/V_0$
AgCl (NaCl → CsCl)	11	-0.0714
AgBr (NaCl → CsCl)	17	-0.0591
AgI (ZB → NaCl)	0.6	-0.1967
AgI (NaCl → CsCl)	49	-0.0277
AgI (NaCl →β-Sn)	46	-0.0208

AgBr and AgI. The c/a ratio varied from 0.5 for smaller volumes, to 1.0 for larger volumes. For AgBr, it is unfavored with respect to the CsCl structure (Fig. 2). For AgI, it appears more competitive, especially above 40 GPa, and we obtain a NaCl → β-Sn transition pressure which is slightly lower than our number for the NaCl → CsCl transition (Fig. 3 and Table II). However, it is still much larger than the experimental 9.7 GPa, which means β-Sn is not a good candidate structure for the phase above the transition.

The NiAs structure is a layered structure, with two-dimensional close-packed layers which are stacked on top of each other, in the order: $AbAcAbAc\ldots$ where the letters designate the three hexagonal sites A, B, and C and small letters are used to distinguish between the two atomic types. The unit cell contains four layers, $AbAc$, which are repeated periodically in the c direction. It has been found experimentally at high pressures in AlAs.[29] For AgBr, and a volume of 300 a.u., we have optimized both the internal parameter u and the lattice parameter c/a. The optimal value of u is 0.25, which makes the Ab (and Ac) interlayer spacing the same as the bA (and cA). We have kept this value of u for all other calculations. Silver atoms prefer the A sites. The optimal value of c/a depends on the volume. It is found to lie between 1.40 and 1.50, increasing with decreasing volume, for pressures below approximately 30 GPa. The NiAs curves are close to their homologous rocksalt ones, but always higher up in energy, so that we can eliminate the NiAs structure as a possible high-pressure phase for the silver halides. To avoid cluttering Figs. 1, 2, and 3, we have not included in them our results for the NiAs structure.

The cinnabar structure has been suggested by Schock and Jamieson[7] as an alternative possibility for the high-pressure phase of AgCl and AgBr. It has been found in compounds which are close to the ionic/covalent border like *cinnabar* itself (HgS), under atmospheric conditions,[4] and CdTe, under pressure.[30] It has also been predicted by first-principles calculations for ZnS (Ref. 31) and ZnTe.[32] It is a hexagonal structure, which can also be viewed in terms of consecutive close-packed planes. Figure 4 shows a projection of its unit cell, which contains six atoms, onto these planes. The lattice vectors $\vec{l_1}$ and $\vec{l_2}$ ($l_1=l_2$ with $l_i \equiv |\vec{l_i}|$), lie within a same plane and the angle between them is $2\pi/3$. The third lattice vector, $\vec{l_3}$ (in general $l_3 \neq l_1$), points perpendicular, along what is usually known as the c axis. We also define an auxiliary vector, $\vec{l'}$, which lies within the $\vec{l_1}\,\vec{l_2}$ plane, at an angle of $2\pi/3$ with both of these vectors. There are six planes inside the unit cell, separated by a distance $l_3/6$, with alternating atomic types. So each of the six atoms shown lies in its own plane, at the height shown in units of l_3 (Fig. 4). To improve on the understanding of the cinnabar structure, imagine first that these atoms remain on their respective plane, but are placed directly above each other, in the center of Fig. 4 (at the origin of $\vec{l_1}$ and $\vec{l_2}$), irrespective of atomic type. This is of course no longer the general cinnabar structure. To (re)construct Fig. 4, from this starting point, consider first that one planar close-packed lattice, say a silver plane, is rigidly displaced in the $\vec{l_1}$ direction, by a distance ul_1. The next silver plane (at a distance $l_3/3$ above) is then displaced by the same amount, but along a new direction $\vec{l'}$. Finally, the third silver plane is rigidly displaced, also by ul_1, in the $\vec{l_2}$ direction. The fourth silver plane is displaced as the first, so that no more silver planes need to be considered. In a similar way, three halide planar lattices are displaced along $\vec{l_1}$, $\vec{l'}$, and $\vec{l_2}$, but by an independent distance which is vl_1. Such a construction leads naturally to a threefold screw axis coincident with the $\vec{l_3}$ (usually c) axis. Notice that the unit cell is described by the two hexagonal lattice parameters, l_1 and l_3, and the internal coordinates u and v. For a fixed volume, there are three degrees of freedom. Each atom is sixfold coordinated by atoms of the other type, with three different distances in general (three different pairs of neighbors in the first coordination shell). The space group, $P3_12$, is generated by the three screw rotations (including the identity) and a rotation by π, besides lattice translations. There is no inversion symmetry. When $u=v=2/3$, however, the structure becomes centrosymmetric. The silver and halide layers are now organized in the rocksalt sequence: $AcBaCbAcBaCb\ldots$, but the cubic unit cell has been distorted in the [111] direction, with rhombohedral symmetry (or trigonal). Such a structure can be described more economically with the three linearly independent lattice vectors,

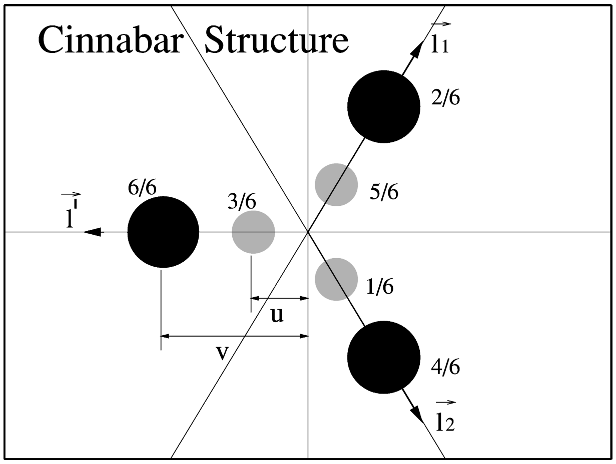

FIG. 4. Projection of the hexagonal unit cell for the cinnabar structure onto a plane perpendicular to the c axis. The lattice vectors $\vec{l_1}$ and $\vec{l_2}$, which lie in the plane of the figure, are shown. The angle between them is $2\pi/3$. A third lattice vector, $\vec{l_3}$, exists perpendicular to the plane, along the c axis. A basis, with six atoms, is also shown. We have chosen it so that two atoms lie above $\vec{l_1}$, two lie above $\vec{l_2}$ and two above a third (auxiliary) vector $\vec{l'}$, which is at an angle of $2\pi/3$ with $\vec{l_1}$ and $\vec{l_2}$, in the plane of the figure. The height of the six atoms is shown in units of l_3. Three atoms, of the "light" kind, lie at a distance ul_1 ($l_i \equiv |\vec{l_i}|$) from the center and the other three, of the "dark" kind, at an independent distance vl_1. Notice the screw axis coincident with the $\vec{l_3}$ axis.

$$\vec{a_1}=\left(\sqrt{\frac{3}{2}}a,\ \frac{1}{2}a,c\right),$$

$$\vec{a_2}=\left(-\frac{\sqrt{3}}{2}a,\ \frac{1}{2}a,c\right),$$

$$\vec{a_3}=(0,-a,c), \tag{4.1}$$

where $\sqrt{3}a$ is the distance between nearest neighbors in the close-packed planes and c is the distance between planes of

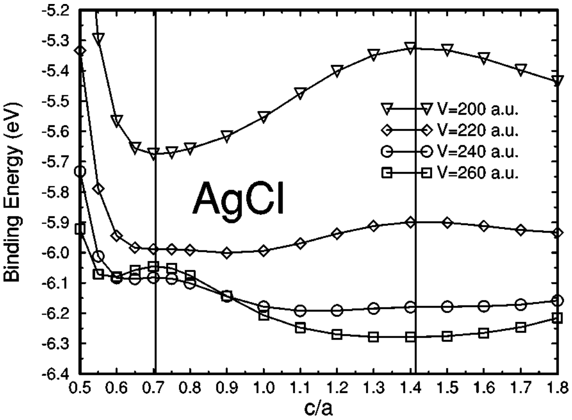

FIG. 5. Calculated binding energies plotted against c/a, for four different volumes V of the rhombohedral cell, for AgCl. This is a special case of the cinnabar structure of Fig. 4 with $u=2/3$ and $v=2/3$. For $c/a=\sqrt{2}$, we have the rocksalt structure and for $c/a=1/\sqrt{2}$ we have the CsCl structure. The appearance of an instability of the rocksalt structure for a volume of 240 a.u. with respect to a rhombohedral distortion is clearly seen. The solid curves are a guide to the eye.

the same atomic type. With these conventions, $a=l_1/\sqrt{3}$ and $c=l_3/3$ $(c/a=1/\sqrt{3}l_3/l_1)$. There are only two atoms in the basis, with positions which are pinned by symmetry. So that for a given volume, only the c/a ratio is left free. At the special value $c/a=\sqrt{2}$, the cubic rocksalt structure emerges and for $c/a=1/\sqrt{2}$ we obtain the simple cubic CsCl arrangement.

We have explored the three-dimensional cinnabar parameter space at constant volume, in search of minima, for AgCl, AgBr, and AgI. For two volumes of AgCl and three volumes of AgBr, our explorations were quite extensive and the special rhombohedral point, $u=2/3$ and $v=2/3$, was found to be optimal for different values of l_3/l_1. For other volumes, we checked only that the rhombohedral point was a relative minimum. This relative minimum condition was also checked for a few volumes of AgI.

Given the above results, Figs. 5 and 6 show our LDA curves for $E=E(V,c/a)$, as c/a is varied at constant V, for rhombohedral AgCl and AgBr. For proper convergence, we have found it necessary, in these calculations, to use a finer grid inside the Brillouin zone, for k-point summation, with $q_1q_2q_3=666$. For large volumes, the energy minimum, with respect to c/a, is clearly located at $c/a=\sqrt{2}$, which is the rocksalt point. Similarly, for small volumes, a clear minimum is seen at $c/a=1/\sqrt{2}$, which is the CsCl point. However, for intermediate volumes, one finds minima which surprisingly lie at values of c/a which are volume dependent and interpolate between the two extremes. Furthermore the curves are very flat, indicating that one of the elastic constants is softening. Since the rocksalt and CsCl (cubic) points are particular cases of the general rhombohedral arrangement, when the optimal value of c/a lies between $1/\sqrt{2}$ and $\sqrt{2}$, a rhombohedral distortion of AgCl and AgBr is preferred to either cubic phase. The rocksalt cube is continuously compressed, along the [111] direction, ''down'' to the CsCl point. Because our minima are very shallow, we have verified that they remain when the cutoff energy is increased up to 100 Ry. We have furthermore checked that such a compression is stable with respect to a GeTe-like deformation (see, for example, Ref. 33, and references therein), which breaks the rhombohedral inversion symmetry.

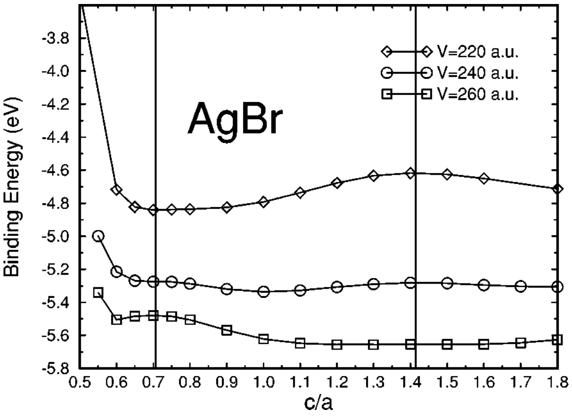

FIG. 6. Calculated binding energies plotted against c/a, for three different volumes V of the rhombohedral cell, for AgBr. The solid curves are a guide to the eye.

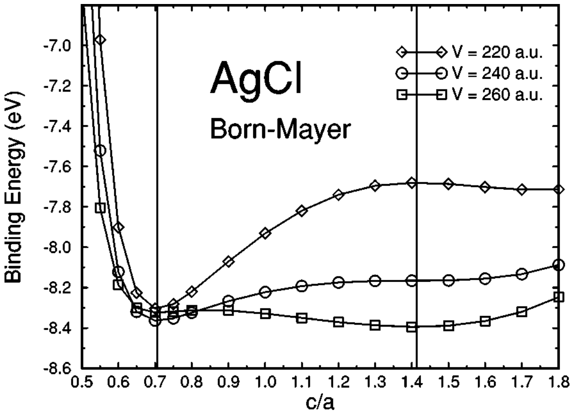

FIG. 7. Calculated binding energies plotted against c/a, for three different volumes V of the rhombohedral cell, for a Born-Mayer model of AgCl. The solid curves are a guide to the eye. The behavior is completely different from the corresponding LDA curves, showing that the ionic interatomic potential cannot describe subtle hybridizations occurring in the silver halides.

In order to gain some insight into this unusual behavior, it is helpful to consider the simple Born-Mayer model for the silver halides. In this model, a full silver $5s$ electron is transferred onto the halide center, leaving behind a pointlike hole. Electrostatic binding forces are then stabilized by a pseudo-hard-core exponential repulsive term $\lambda\exp(-r/\rho)$. This is generally regarded as a fair representation of ionic crystals. We fit the two parameters λ and ρ to the experimental values of the equilibrium lattice constant and the bulk modulus for AgCl. Within this model, we find that the optimal values for the internal parameters u and v, for the cinnabar structure, are also the values of 2/3, which, as stated above, degenerate the cinnabar structure into the rhombohedral structure, of higher symmetry. This means that the silver halides behave ionically in avoiding the cinnabar structure. Figure 7 shows curves like those of Figs. 5 and 6, but which are calculated with the simple ionic model of Born and Mayer. We observe

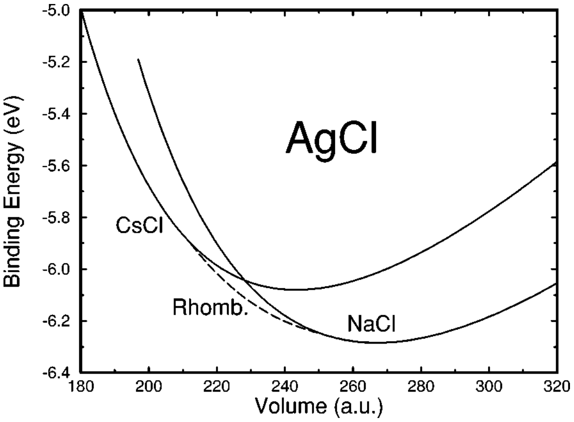

FIG. 8. AgCl: Calculated binding energy for the rocksalt and CsCl structures, in solid lines. We find that these structures are connected by an intermediate rhombohedral curve, as shown in the dashed line, instead of the usual common tangent.

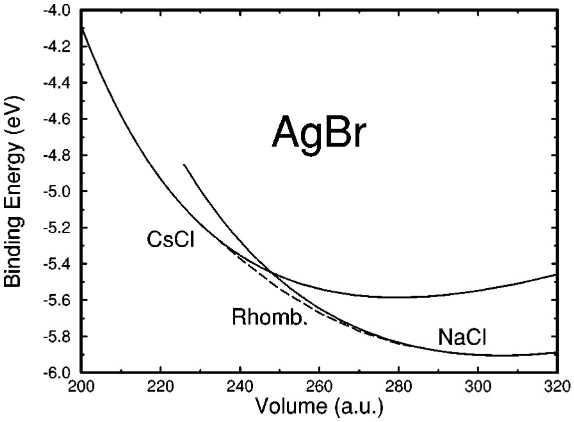

FIG. 9. AgBr: Calculated binding energy for the rocksalt and CsCl structures, in solid lines. We find that these structures are connected by an intermediate rhombohedral curve, as shown in the dashed line, instead of the usual first-order common tangent.

again the two extreme cases — NaCl and CsCl — but nothing in between. There are no intermediate minima in this model. We checked by performing first-principles calculations for NaCl that, in an ionic crystal like rocksalt itself, the LDA description does not predict intermediate minima, and thus the Born and Mayer model works better. The rhombohedral compression of the silver halides, must therefore be attributed to the hybridization between the halide *p* and silver *d* states, which results in a non-negligible covalent bonding.

If we now recall Figs. 1 and 2, a rhombohedral compression of AgCl and AgBr means that instead of a common tangent joining the rocksalt phase to the CsCl phase, these are connected by an intermediate curve at lower energy. This is what is shown in Figs. 8 and 9. The rhombohedral structure is therefore the most favorable structure studied in an intermediate range of pressures, for AgCl and AgBr.

Figure 10 shows the computed equation of state, in the form $V = V(P)$, from $E = E(V)$, through the relation $P \equiv -\partial E/\partial V$, which defines the pressure. Figure 10 also contains the low-pressure measurements of Vaidya and Kennedy[34] for $P(V)$ (squares). The low-pressure 0.4 GPa transition of AgI from the zinc-blende to rocksalt structures is well described. In the compression of AgCl and AgBr, in the rocksalt phase, our calculations predict a harder crystal, but as mentioned before, there is significant softening of those crystals with temperature, while our calculations should describe the low-temperature regime. The dashed lines show the equation of state that would be obtained if we had only considered the usual ionic NaCl → CsCl transition. For AgBr and AgI, this is predicted to occur at pressures much higher than the observed P_c (arrows in Fig. 10), for transitions from the NaCl structure into a not yet well determined structure. For AgCl and AgBr, Fig. 10 also shows the continuous evolution through the rhombohedral intermediate phase, in solid lines. These curves follow the rocksalt and CsCl phases, which are special cases of the general rhombohedral structure, at low and high pressures, respectively. The onset of the rhombohedral compression is calculated at 5 GPa for AgCl and 7.5 GPa for AgBr, below the experimental transition pressures. The transition is fully completed at 18 GPa for AgCl and 32 GPa for AgBr. For AgI, we have determined the rhombohedral compression to begin at 40 GPa, a pressure at which the enthalpy of this phase is almost the same as the β-Sn structure. As this should not be relevant for the transition observed around 9.7 GPa, we have not performed the computationally expensive calculations that would be necessary to determine an equation of state for AgI that included the rhombohedral phase.

In light of our results, let us now examine possible scenarios for the behavior of the silver halides under pressure. Our calculations suggest that it is very likely that there is at

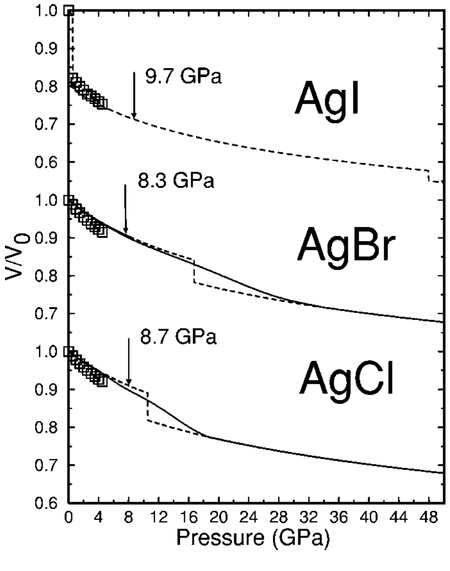

FIG. 10. Change of the relative volume of AgCl, AgBr, and AgI with increasing pressure. The squares represent experimental results (Ref. 34). The dashed line represents the results of this work under the supposition of a first-order transition into the CsCl phase. The solid lines show the continuous rhombohedral compression of AgCl and AgBr which we predict to be more favorable. For AgI, this is not shown though we have calculated the onset of such a compression to occur at 40 GPa. The arrows mark the experimentally observed transition pressures. The first transition in AgI is from zincblende or wurtzite to rocksalt (experimentally $P_c = 0.4$ GPa) and is correctly described by the calculations.

least one intermediate structure between the rocksalt phase and the CsCl phase in AgI. We were not able to find a good candidate for that intermediate phase, but we can say that it is probably not one of those considered in this paper. For AgCl and AgBr, we found an instability related to the softening of an elastic constant in the pressure ranges where a transition is seen to occur, but not on top of the experimental value. From Fig. 5, we can tell that although there is no discontinuous change in volume, from the low-pressure rocksalt to the CsCl structure, the c/a parameter could change quite fast. We did not include in our calculations zero-point motion or temperature effects. But the basic occurrence of an instability should be reliably predicted by our calculations. It is possible that this instability is exactly rhombohedral and that Schock and Jamieson have observed a discontinuous evolution from the rocksalt phase into an intermediate rhombohedral point because their samples could not be compressed sufficiently slowly. Indeed, the real evolution of crystalline samples under pressure cannot be guaranteed to proceed quasistatically (for example hysteresis is common). Schock and Jamieson[7] have measured a hexagonal phase on the high-pressure side of a transition. They have conjectured it to be the cinnabar phase with values of u and v similar to what is found in HgS itself, but do not mention a calculation of x-ray line intensities corresponding to the special rhombohedral case $(u=v=2/3)$. It would be interesting to check this. With our conventions [see Eq. (4.1)], Schock and Jamieson measure $c/a\approx 1.0$ (for AgCl and AgBr) which would pertain to such a rhombohedral point between the rocksalt phase and the CsCl phase.

New experimental work on the high-pressure phases of the silver halides, would be very important for the final solution of this puzzle. We would be particularly interested in the examination of the possibility that the structures above ≈ 8 GPa, for AgCl and AgBr, are related to the predicted rhombohedral instability.

V. CONCLUSION

We have shown that the LDA, pseudopotentials, and plane waves, with the inclusion of the silver d electrons, give fairly accurate structural parameters for the ground states of silver halides, giving also the right structural preferences, as for better studied alkali halides and semiconductors. Our results for the transition between the zinc blende and rocksalt phases for AgI is in fair agreement. We also find that transitions observed around $8-10$ GPa, in the silver halides should not be from the rocksalt to the CsCl structure as proposed by Slykhouse and Drickamer,[6] but to noncubic structures as proposed by Schock and Jamieson. We find an instability of the rocksalt phase of AgCl and AgBr with respect to a rhombohedral structure, associated with a softening of one of the elastic constants of the rocksalt phase at pressures just below where the experimental transitions are observed. The observed transition could be associated with this instability. For AgI, we did not identify a candidate structure into which the rocksalt phase transforms, but our calculations suggest that it is not CsCl.

ACKNOWLEDGMENTS

We are grateful to T. Gasche for a careful reading of the manuscript and helpful comments. Some of the computation required for this work was performed thanks to NSF Grant No. DMR-9417755. G.S. Nunes was supported by JNICT/PRAXIS XXI/BD-3823 and by the U.S. Department of Energy, under Contract No. DE-AC02-76CH00016. This work was also supported by JNICT Grant No. STRDA/C/CTM/597/92, PRAXIS/2/2.1/FIS/467/94, and NATO collaborative Grant No. 920627.

---

[1] J. F. Hamilton, Adv. Phys. **37**, 359 (1988).

[2] B. E. Mellander, Phys. Rev. B **26**, 5886 (1982).

[3] J. C. Phillips, Rev. Mod. Phys. **42**, 317 (1970).

[4] R. W. G. Wyckoff, *Crystal Structures* (Wiley, New York, 1963).

[5] P. W. Bridgman, Proc. Am. Acad. Arts Sci. **74**, 1 (1945).

[6] T. E. Slykhouse and H. G. Drickamer, J. Phys. Chem. Solids **7**, 207 (1958).

[7] R. N. Schock and J. C. Jamieson, J. Phys. Chem. Solids **30**, 1527 (1969).

[8] J. E. Maskasky, Phys. Rev. B **43**, 5769 (1991).

[9] D. A. Keen and S. Hull, J. Phys.: Condens. Matter **5**, 23 (1993).

[10] B. L. Davis and L. H. Adams, Science **146**, 519 (1964).

[11] R. C. Hanson, T. A. Fjeldly, and H. D. Hochheimer, Phys. Status Solidi **70**, 567 (1975).

[12] B. M. Riggleman and H. G. Drickamer, J. Chem. Phys. **38**, 2721 (1963).

[13] F. Kirchhoff, J. M. Holender, and M. J. Gillan, Phys. Rev. B **49**, 17 420 (1994).

[14] J. R. Chelikowsky, Phys. Rev. B **35**, 1174 (1987).

[15] D. C. Gupta and R. K. Singh, Phys. Rev. B **43**, 11 185 (1991).

[16] G. S. Nunes, P. B. Allen, and J. L. Martins, Solid State Commun. (to be published).

[17] P. Hohenberg and W. Kohn, Phys. Rev. **136**, B864 (1964).

[18] W. Kohn and L. J. Sham, Phys. Rev. **136**, A1133 (1965).

[19] D. M. Ceperley and B. J. Alder, Phys. Rev. Lett. **45**, 566 (1980).

[20] J. Perdew and A. Zunger, Phys. Rev. B **23**, 5048 (1981).

[21] J. L. Martins and M. L. Cohen, Phys. Rev. B **37**, 6134 (1988).

[22] N. Troullier and J. L. Martins, Phys. Rev. B **43**, 1993 (1991).

[23] L. Kleinman and D. M. Bylander, Phys. Rev. Lett. **48**, 1425 (1985).

[24] X. Gonze, R. Stumpf, and M. Scheffler, Phys. Rev. B **44**, 8503 (1991).

[25] H. J. Monkhorst and J. D. Pack, Phys. Rev. B **13**, 5188 (1976).

[26] F. D. Murnaghan, Proc. Natl. Acad. Sci. USA **30**, 244 (1944); O. L. Anderson, J. Phys. Chem. Solids **27**, 547 (1966).

[27] W. Hidshaw, J. T. Lewis, and C. V. Briscoe, Phys. Rev. **163**, 876 (1967).

[28] P. Lawaetz, Phys. Rev. B **5**, 4039 (1972).

[29] R. G. Greene, H. Luo, T. Li, and A. L. Ruoff, Phys. Rev. Lett. **72**, 2045 (1994).

[30] M. I. McMahon, R. J. Nelmes, N. G. Wright, and D. R. Allan, Phys. Rev. B **48**, 16 246 (1993).

[31] A. Nazzal and A. Qteish, Phys. Rev. B **53**, 8262 (1996).

[32] G. Lee and J. Ihm, Phys. Rev. B **53**, 7622 (1996).

[33] K. M. Rabe and J. D. Joannopoulos, Phys. Rev. B **36**, 6631 (1987).

[34] S. N. Vaidya, and G. C. Kennedy, J. Phys. Chem. Solids **32**, 951 (1971).

[35] D. S. Tannhouser, L. J. Bruner, and A. W. Lawson, Phys. Rev. **102**, 1281 (1956).

[36] P. W. Atkins, *Physical Chemistry* (Oxford University Press, Oxford, 1990).

[37] R. C. Hanson, T. A. Fjeldly, and H. D. Hochheimer, Phys. Status Solidi A **70**, 567 (1975).

[38] R. K. Singh and P. Khare, Phys. Status Solidi B **103**, 337 (1981).